

## NUMERICAL PREDICTION OF DILUTE PARTICULATE FLOWS IN HORIZONTAL AND VERTICAL DUCTS

Benny KUAN<sup>1</sup> and M. Philip SCHWARZ<sup>2</sup>

<sup>1</sup> CRC – Clean Power from Lignite, Mulgrave, Victoria 3170, AUSTRALIA

<sup>2</sup> CSIRO Minerals, Clayton, Victoria 3169, AUSTRALIA

### ABSTRACT

Two-phase turbulent flow calculations are performed using a commercial Computational Fluid Dynamics (CFD) software CFX-4.4. With the aid of available experimental data, the work is aimed at exploring a range of issues concerning the application of CFD to model gas-solid flows having different cross-section geometry and flow orientation. In order of increasing flow complexity, the present study first looks at the importance of drag coefficient and inlet conditions to particle track calculations in a vertical duct. The same analysis is then performed for two-phase horizontal flows, where gravitational settling starts to exert a stronger influence over the distribution of particles within the flow domain. All computations carried out take into account the effect of Saffman force and particle-wall collisions. Although both flows considered could be reasonably regarded as two dimensional, knowledge gained from such a study is expected to be also applicable to three-dimensional gas-solid flow problems.

### NOMENCLATURE

e	restitution coefficient
d	particle diameter
<b>F</b>	force vectors acting on particle surface
H	channel height
k	turbulence kinetic energy
$L_p$	particle mass loading
m	particle mass
<b>u</b>	velocity vector
U	horizontal velocity
V	vertical velocity
W	channel width
$\alpha$	particle impact angle
$\varepsilon$	turbulence dissipation rate
$\mu$	gas dynamic viscosity
$\omega$	specific turbulence dissipation rate

### INTRODUCTION

Dilute gas-solid flows prevail in a wide range of engineering applications, one of which is pneumatic conveying of pulverised fuel (pf) in coal-fired power stations. Before coals are burnt at the boilers, they are first pulverised into particles of various sizes by the mill and then delivered to downstream furnaces by flue gases under different, sometimes unknown, flow conditions. In such an industrial flow, a thorough on-line measurement is usually very difficult and expensive to perform. In laboratories, numerous experimental studies have been

carried out by various researchers in the past on pneumatic conveying flow phenomena (Fan et al., 1997), however the majority of them tend to focus on cases with mass loading ratios  $L_p$  above 1.0 and particle sizes greater than 100  $\mu\text{m}$ . Such conditions are distinctively different from the operating environment that normally prevails in a power plant mill-duct system, ie.  $L_p = 0.1$  and particle sizes between 45  $\mu\text{m}$  and 80  $\mu\text{m}$  (Manickam *et al.*, 2001). In view of this apparent lack of published studies on dilute particulate flows involving fine suspended particles, design of the mill-duct network for coal-fired power plants has so far been largely based on empiricism.

With the advent of high-speed digital computers, engineers nowadays could resort to Computational Fluid Dynamics (CFD) for a better understanding of the pf delivery process before any future plant optimisation is carried out. Unfortunately, for many complex flows, CFD analysis can only offer a qualitative, rather than a quantitative, prediction of the flow behaviour. This is because the majority of the numerical models used in CFD were created using flow data that are sometimes only remotely representative of the real industrial flow.

Model validation is therefore essential to ensure the numerical models are capable of solving industrial flow problems that have not been extensively studied by the scientific community.

The present investigation focuses on an evaluation of dilute gas-solid flows in straight ducts, which are extensively used in mill-duct networks. The two flow conditions considered are vertical upward flow through a circular-sectioned pipe (Maeda *et al.*, 1980) and horizontal channel flow with a width-to-height ratio (W/H) of 10 (Kussin and Sommerfeld, 2002). Unlike in pure-gas flows where the influence of gravity on gas dynamics is negligible, motion of the dispersed solids is strongly affected by gravitational settling. Consequently, one should expect the solid distributions in the two flows to vary drastically.

In the process of obtaining the final numerical prediction, low Reynolds number two-equation models are applied for solving gas phase turbulence. For the solid phase, particle tracks are calculated through a Lagrangian approach taking into account only one-way coupling effect. Particle velocity profiles are compared against the measured data. Where possible, particle number distributions are also presented.

## FLOW CONDITIONS CONSIDERED

### Vertical upward pipe flow

Maeda *et al.* (1980) experimentally investigated gas-solid flow in a vertical pipe. In their experiment, an upward flow system had been set up to facilitate Laser-Doppler Anemometry (LDA) measurements of solid velocity as well as hot wire anemometer measurement of gas-phase velocity and turbulence quantities. A 4 m straight circular section pipe of unknown material (presumably plexiglass) with internal diameter of 56 mm was fitted downstream of an upward bend. Spherical glass powder with a mean diameter of 136  $\mu\text{m}$  was introduced into the gas flow at a solid mass loading ratio  $L_p$  of 30%. At pipe Reynolds number of  $2.0 \times 10^4$ , the experimenters confirmed that the mean axial velocities for the single-phase flow have the same profile as that in a fully-developed turbulent flow. The corresponding mean air velocity was 5.7 m/s.

### Horizontal channel flow

Calculations are also performed for a gas-solid flow through a horizontal channel. The flow configuration studied corresponds to a flow experiment conducted by Kussin and Sommerfeld (2002) who tested a 6 m horizontal channel with a width (W) of 350 mm and a height (H) of 35 mm. Owing to its large width-to-height ratio (W/H), the experimenters were satisfied that measurements made at the channel's centre plane were reasonably free from wall effects, and hence the results represent two-dimensional flow behaviours.

The upper and bottom walls were made from stainless steel plates that could be replaced with plates of different surface finish to facilitate a more in-depth study on the effect of wall roughness. Spherical glass beads of 100  $\mu\text{m}$  were injected into the channel to attain a solid mass loading ratio of 10%. The average air velocity ( $U_b$ ) was 19.7 m/s.

## MATHEMATICAL MODELS

### Gas-Phase

Local mean gas flow properties, such as velocity and turbulent kinetic energy, are calculated numerically by solving a set of Reynolds-averaged Navier-Stokes partial differential equations using the commercial CFD software CFX-4.4. Reynolds stresses are expressed algebraically as a linear expansion of the Boussinesq approximations. To facilitate the application of fine near-wall meshes, low Reynolds number turbulence (LRN) models, which solve either turbulence dissipation rate  $\varepsilon$  (k- $\varepsilon$  model) or specific dissipation rate  $\omega$  (k- $\omega$  model), are utilised. Full detail on the turbulence models used can be found in CFX-4 Flow Solver User Guide (AEA Technology, 2000).

### Solid-Phase

Instantaneous positions and velocities of the dispersed phase are solved from a set of ordinary differential equations following a Lagrangian particle tracking methodology. Motion of particles suspended in a continuous fluid is determined by numerically integrating the equations of motion for the dispersed phase in a fluid flow. The equation of particle motion may be expressed as

$$m_p \frac{du_p}{dt} = F_D + F_g + F_{pg} + F_A + F_{sl} \quad (1)$$

where subscript p represents particle properties and subscripts D, g, pg, and A respectively denote force components arising from drag, gravity, flow pressure gradient, added mass effect, and Saffman shear-lift force. A detailed description of mathematical models for the force components considered in (1) is available from Fan and Zhu (1998), and Huber and Sommerfeld (1998).

The particle drag coefficient  $C_D$  is estimated from a widely-applied mathematical expression (Wang *et al.*, 1998):

$$C_D = \frac{24}{Re_p} \left( 1 + 0.15 Re_p^{0.687} \right), \quad Re_p < 1000 \quad (2)$$

$$C_D = 0.44, \quad , \quad Re_p \geq 1000$$

where  $Re_p$  is particle Reynolds number based on particle slip velocity, particle diameter  $d_p$  and gas density.

In order to solve the equation of motion (1) for every particle track in the flow domain, instantaneous fluid velocity components at all particle locations need to be determined in advance. It is through the inclusion of these instantaneous fluid velocity components that the effects of turbulence are taken into account in the calculation of particle motions. The present work adopts a classical stochastic approach by Gosman and Ioannides (1981) for the estimation of fluid fluctuating velocities. Subsequent particle track integration is carried out over an interaction time that is the minimum of two time scales, namely, eddy lifetime and particle transit time.

### Particle-wall collision with wall roughness

As was mentioned previously, even though both of the considered experiments utilised glass beads as the solid-phase, the confining walls in each case were made from materials of different surface roughness. The particle-wall collision model should, thus, be modified to reflect this in the calculation. The present study adopts Sommerfeld and Huber (1999)'s model for wall roughness, and Matsumoto and Saito (1970)'s model for particle-wall collision. The wall-roughness model was developed on the basis of a series of wall collision experiments involving glass particles and walls of different material.

To introduce the effect of wall roughness into the particle-

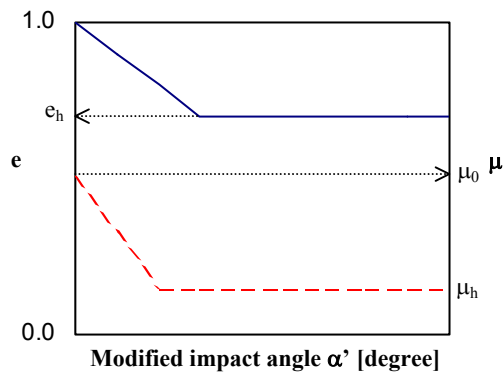


**Figure 1:** Assumed variation of  $e$  and  $\mu$  with modified impact angle

**Table 1:** Wall-roughness parameters for 100 $\mu$ m spheres

$e_h$	$\alpha e$ [degree]	$\mu_0$	$\mu_h$	$\alpha_\mu$ [degree]	$\Delta\gamma$ [degree]
Glass particle + steel wall					
0.7	22	0.5	0.15	20	6.5
Glass particle + plexiglass wall					
0.73	18	0.4	0.15	27	3.8

wall collision model, Sommerfeld and Huber modified the 'smooth-wall' impact angle  $\alpha$  with a random component characterising the presence of a rough wall:

$$\alpha' = \alpha + \Delta\gamma\xi \quad (3)$$

where  $\Delta\gamma\xi$  represents a random component sampled from a Gaussian distribution function.  $\xi$  is Gaussian random number with zero mean and standard deviation of unity.  $\Delta\gamma$  is standard deviation of wall roughness angle.

They then allowed both coefficients of restitution  $e$  and friction  $\mu$  to vary with the modified impact angle  $\alpha'$  via two semi-empirical relations that are graphically depicted in Figure 1. The characteristic values for models developed for 100  $\mu$ m glass spheres are provided in Table 1.

## RESULTS

### Vertical upward pipe flow

A series of two-phase flow calculations are run to examine the influence of drag coefficient  $C_D$  and inlet conditions on the predicted particle motion. All computations are based on a five-block mesh system that represents a 2 m section of the tested pipe. A total of 381,000 cells have been used with a minimum wall spacing less than  $y^+ = 0.3$ . Fine cell resolution is used near the wall so that the low Reynolds number  $k-\epsilon$  turbulence model can be applied. Fully-developed turbulence is assumed in accordance with the experimental observation.

Under the same flow condition, an earlier numerical study revealed that the calculated particle motion, involving two-way coupling effects, exhibits negligible response to solid mass loading ratios within the range  $0.1 < L_p < 0.3$ . Apart from  $L_p$  insensitivity, the study also established a numerical solution that is independent of mesh sizes and turbulence models. In view of this, all flow predictions presented in the following consider only one-way coupling effects and are based on the same mesh system that will lead to a grid-independent solution.

### Effect of drag coefficient

Calculated and measured particle axial velocity profiles are compared in Figure 2a with  $V_{g,c}$  being the measured centreline gas velocity and  $V_p$  the particle velocity. While the measured profile represents time-mean particle velocities, the predicted profiles are lines-of-best-fit based on 10,000 calculated particle tracks passing through  $z/D = 35$ . The result indicates  $C_D$  as a major parameter that critically affects the predicted particle motion in the core region. Further, the standard equation for  $C_D$  (2) needs to be reduced significantly if the calculated profile at the duct centre ( $r/R=0.0$ ) is to match the measured distribution.

Away from the core but well outside the near-wall region ( $0.4 < r/D < 0.9$ ), all three calculations substantially under-predict particle's axial velocities. With reference to Maeda *et al.* (1980)'s measurement, this corresponds to an area of increasing turbulence intensity and a much higher level of  $C_D$  seems to be necessary to raise the predicted profiles.

Such an observation is supported by various published studies, including Brucato *et al.* (1998) and Uhlherr and Sinclair (1970). Their experiments indicated a strong correlation between higher gas turbulence and a significant increase in particle drag coefficients above the standard curve (2).

Apart from the solid-phase velocity distribution over the pipe cross-section, drag coefficients also strongly affect particle acceleration in the direction of the flow. As is shown in Figure 2b where particle velocity distributions along the duct centreline ( $V_{p,c}$ ), and near the wall ( $V_{p,w}$ ) are plotted, application of 100% $C_D$  forces particles at the core to accelerate excessively towards duct exit. At  $z/D = 35$ , particles are travelling at an axial velocity 8.2% higher

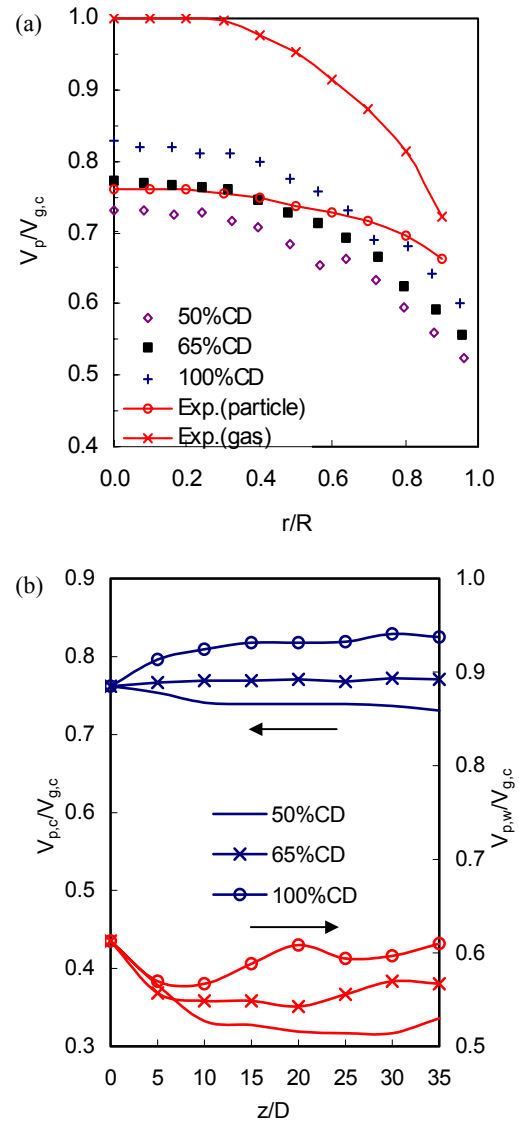


**Figure 2:** Dependence of normalised particle velocity distributions on  $C_D$  (a) radial profile; (b) axial profile

than the measured value. On the other hand, reducing  $C_D$  to 65% of the standard value causes the particle to maintain at roughly the same axial velocity throughout the duct.

Regardless of particle's final velocity in the duct, particulate flow at the core appears to stabilise into a steady state as early as  $z/D = 10$ . The same, however, does not happen near wall because the particles in this region are also under the combined influence of particle-wall collision and Saffman force, which respectively act to slow down and redistribute fast particles towards the wall.

### Inlet sensitivity

Three different inlet velocity profiles for the particles are tested in separate calculations to examine their influence on the numerical solutions. Particle's axial velocity distributions across the duct, as well as in the streamwise direction, are respectively presented in Figure 3a and 3b. Results compared in the figure pertain to cases where different velocity profiles are assigned to the particles at the duct inlet:

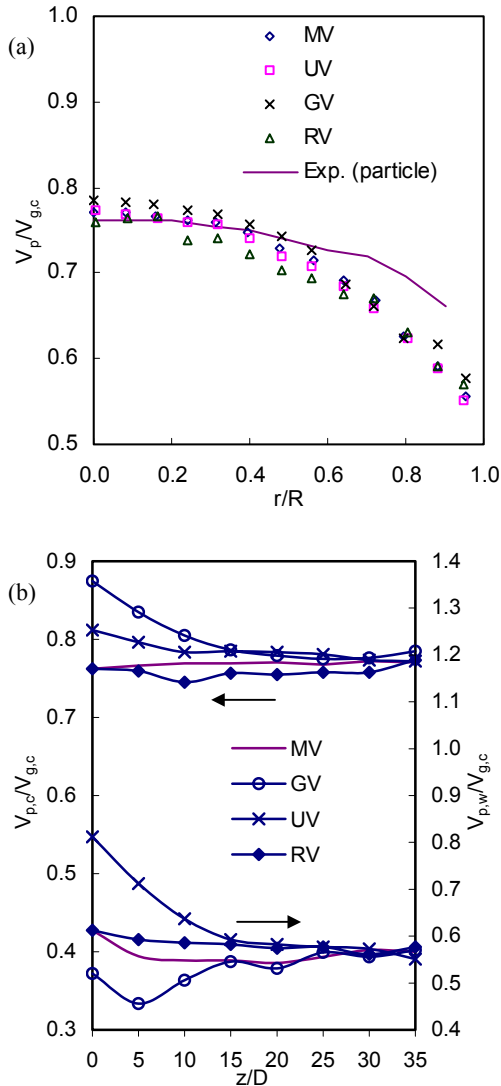


**Figure 3:** The predicted velocity's dependence on particle inlet conditions (a) radial profile; (b) axial profile

1. the measured particle velocity (MV);
2. a uniform velocity (UV) equivalent to the mean air velocity 5.7 m/s;
3. the measured gas velocity (GV); and
4. a variant of MV with an arbitrary transverse velocity component (RV) that is randomised to simulate cross-stream migration of particle tracks due to particle-wall collisions prior to the pipe inlet;

The graph indicates that, when the carrier-fluid is in a fully-developed state, the predicted particle tracks at  $z/D = 35$  are insensitive to the prescribed inlet particle velocities. This is further confirmed in Figure 3b, which depicts streamwise development of particle velocities at the duct core as well as in the near-wall region. Differences amongst the three predicted particle velocities at  $z/D = 35$  are found to be less than 3%.

### Horizontal channel flow

A similar analysis is carried out for the horizontal channel. The computed domain is 1.5 m long and contains  $40 \times 110 \times 90$  cells with a minimum near-wall spacing of  $y^+ = 0.61$ . A low Reynolds number  $k-\omega$  turbulence model is utilised to perform the gas-phase calculations. Again, fully-developed turbulence is assumed within the channel.

Particle motion in a two-phase horizontal channel is distinctively different from that in a vertical pipe, which was examined previously. In the horizontal channel, gravity is acting perpendicular to the main flow, and hence the particles will develop a greater tendency to interact with the lower wall. One should therefore expect the effect of particle-wall collisions to be more pronounced in this flow environment.

### Inlet sensitivity

Unlike the vertical flow where a majority of the particles are expected to travel well clear of the confining walls, particle motion in a horizontal flow may be strongly affected by the presence of frequent particle-wall collisions even before they enter the test section. To reflect this possibility, inlet conditions for the dispersed-phase should incorporate a small and yet random vertical velocity component.

In the present calculation, two sets of inlet velocity profiles have been tested: one that is based on the measured time-mean particle horizontal ( $U_{p,measured}$ ) and vertical ( $V_{p,measured}$ ) velocity; and in the second set, a small component is added to the measured vertical velocity profile to give an instantaneous particle vertical velocity  $v_{in}$ :

$$v_{in} = V_{p,measured} + v'_{p,rms}\zeta \quad (4)$$

where  $v'_{p,rms}$  is the measured rms velocity fluctuation; and  $\zeta$  is a random number sampled from a uniform distribution function between  $-1$  and  $1$ . According to Kussin and Sommerfeld (2002), all particles in the horizontal pipe tend to fluctuate at a uniform mean fluctuating velocity  $v'_{p,rms}$  that is 10% of the average air velocity. The same condition is therefore applied to the calculated particle tracks at the inlet. The inlet conditions discussed above are depicted graphically in Figure 4.

Both calculations are based on the standard  $C_D$  curve (ie.  $100\%C_D$ ) with 10,000 particle tracks, and they are presented in Figure 5 (first two datasets). Figure 5

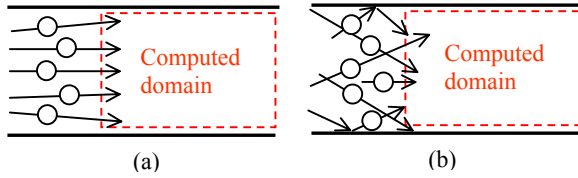


**Figure 4:** Particle inlet conditions tested (a)  $v_{in} = V_{p,measured}$ ; (b)  $v_{in} = V_{p,measured} + v'_{p,rms} \zeta$  ( $U_{p,measured} \gg V_{p,measured}$ )

examines streamwise development of the predicted particle velocities  $U_p$ .

When the calculation ignores any pre-existing particle-wall collisions, Figure 5 shows a downward shift of local

velocity maximum in profiles at  $x/H = 10, 20, 30$  and  $40$ . This suggests a trend that the fast-moving particles at the channel centre are gradually moving towards the lower wall under the influence of gravity further downstream. In contrast, particles that enter the flow domain with a small  $v'_{p,rms}$  component appear to travel at a more stable velocity through the channel.

Particle number distributions ( $C_n$ ) are also calculated and they are normalised by the total number of particles at each station. The results are presented in Figure 6 and it clearly indicates a strong tendency for the predicted particles to settle to the lower wall if they were to enter the flow domain parallel to the wall (Figure 4a). Due to

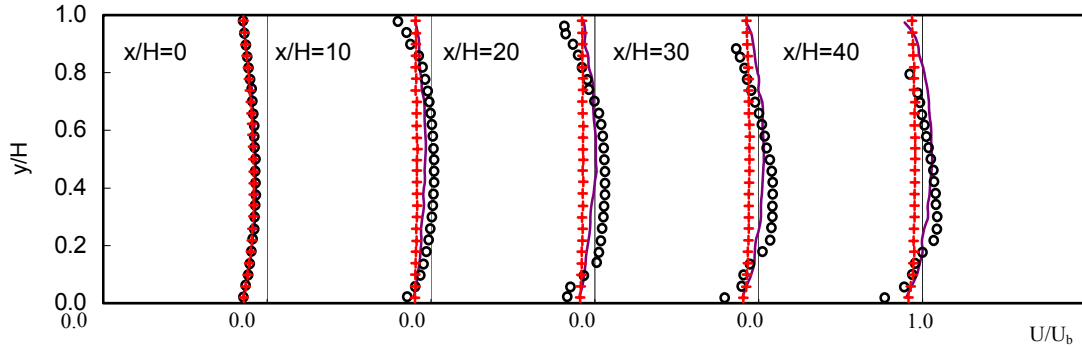


**Figure 5:** Predicted streamwise particle velocity profiles  $U_p$  (o  $v_{in} = V_{p,measured}$  at 100% $C_D$ ;  $\times$   $v_{in} = V_{p,measured} +$  randomised  $v'_{p,rms}$  at 100% $C_D$ ;  $\circ$   $v_{in} = V_{p,measured} +$  randomised  $v'_{p,rms}$  at 20% $C_D$ )

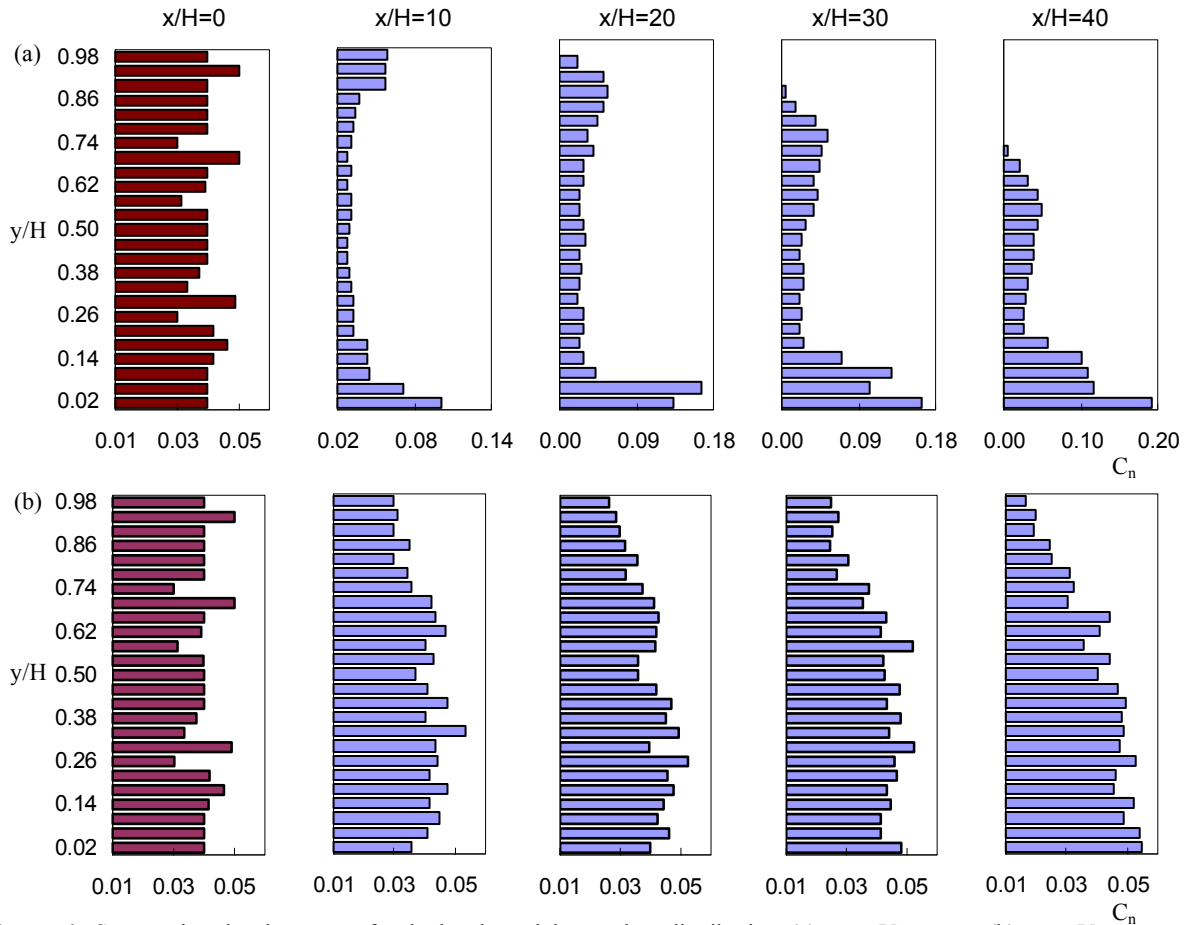


**Figure 6:** Streamwise development of calculated particle number distribution (a)  $v = V_{p,measured}$ ; (b)  $v = V_{p,measured} +$  randomised  $v'_{p,rms}$ )

gravitational settling, particles quickly become scarcer near the top wall as a majority of the particles migrate toward the lower wall, leading to a sharp rise in particle number near the lower wall.

The same tendency, however, is less pronounced when the horizontal inflow condition is changed to that shown in Figure 4b. Consideration of non-negligible upstream particle-wall collisions has led to a more gradual rise in particle number close to the lower wall. This is also found to substantially contribute to a higher upper-wall particle number even at 40H downstream from the inlet.

Although particle number concentration was measured in Kussin and Sommerfeld (2002)'s experiment, their data is not directly comparable to the present result. Nevertheless, the calculated profile obtained with a random  $v'$  at  $x/H = 35$  does bear reasonable qualitative resemblance to the measured particle concentration distribution.

#### **Dependence on drag coefficient**

Apart from the gravitational settling effect, Figure 5 also illustrates that, with the application of the standard drag curve (2), the calculated particles are subject to a moderate acceleration at the core. However, from the limited flow measurement, it is impossible to establish whether the particles would accelerate by flow entrainment or slow down as a result of particle-wall collisions once they pass the measurement location. As was discussed earlier for the vertical pipe flow, such a continual increase in particle velocity may be a result of exceedingly high drag coefficients as given by (2).

Additional calculations are thus performed with an altered  $C_D$  curve (20% of (2)) and assuming non-horizontal particle entry (Figure 4b). This results in a mere 4% increase in predicted particle velocity between  $x/H = 0$  and  $x/H = 40$  (Figure 5). The predicted particle number distributions are not presented, as they and the profiles shown in Figure 6b remain much the same.  $C_D$  is therefore one of the predominant factors that affect particle velocity predictions in horizontal pipes.

#### **CONCLUSION**

A vertical upward flow with circular cross-section and a 2D horizontal flow have been examined numerically in the present study. Comparison with the corresponding experimental measurements reveals that solutions for both flows are sensitive to particle  $C_D$ . In the vertical flow,  $C_D$  needs to be reduced by as much as 35% of the standard value to obtain a good match between the predicted velocities downstream and that upstream at the pipe centre. In the horizontal flow, however, a 20% $C_D$  is necessary to achieve the same effect.

The numerical solution's sensitivity to prescribed inlet conditions has also been evaluated and it is found that particle velocities predicted in a vertically upward turbulent flow field tend to reach the same steady-state downstream flow profile regardless of inlet conditions. In contrast, development of the predicted particle velocity and number distribution in a horizontal flow strongly depends on inlet conditions. A small and randomised cross-stream velocity component is necessary to account for any possible particle-wall collisions upstream of the computed flow domain. This also dampens the influence

of gravitational settling on particles and consequently leads to a more uniform particle distribution in the channel.

#### **ACKNOWLEDGMENTS**

The authors gratefully acknowledge the financial and other support received for this research from the CRC-Clean Power from Lignite, which is established and supported under the Australian Government's Cooperative Research Centre program.

#### **REFERENCES**

- AEA Technology, 2000, Computational Fluid Dynamics Services, *CFX-4 User manual*, Harwell, UK
- BRUCATO, A., GRISAFI, F., and MONTANTE, G., (1998), "Particle drag coefficients in turbulent fluids," *Chemical Engineering Science*, **53(18)**, 3295-3314
- FAN, J., ZHANG, X., CHENG, L., and CEN, K., (1997), "Numerical simulation and experimental study of two-phase flow in a vertical pipe," *Aerosol Science and Technology*, **27**, 281-292
- FAN, L.S., and ZHU, C., (1998), "Principles of gas-solid flows," Cambridge University Press, Cambridge, UK
- GOSMAN, A.D., and IOANNIDES, E., (1981), "Aspects of computer simulation of liquid-fuelled combustors," *AIAA paper no. 81-0323*
- HUBER, N., and SOMMERFELD, M., (1998), "Modelling and numerical calculation of dilute-phase pneumatic conveying in pipe systems," *Powder Technology*, **99**, 90-101
- KUSSIN, J., and SOMMERFELD, M., (2002), "Experimental studies on particle behaviour and turbulence modulation in horizontal channel flow with different wall roughness," *Experiments in Fluids*, **33**, 143-159
- MAEDA, M., HISHIDA, K., and FURUTANI, T., (1980), "Optical measurements of local gas and particle velocity in an upward flowing dilute gas-solids suspensions," *Polyphase Flow and Transport Technology*, presented at the Symposium on Polyphase Flow and Transport Technology, ASME, New York
- MATSUMOTO, S., and SAITO, S., (1970), "Monte Carlo simulation of horizontal pneumatic conveying based on the rough wall model," *Journal of Chemical Engineering of Japan*, **3(2)**, 223-230
- MANICKAM, M., SCHWARZ, M.P., and MCINTOSH, M.J., (2001), "CFD modelling of solids maldistribution in mill-duct flows," *Proceedings of the 7<sup>th</sup> International Conference on Bulk Materials Storage, Handling and Transportation*, Ed M Jones, University of Newcastle: Institution of Engineers Australia, pp. 833-840
- SOMMERFELD M., and HUBER, N., (1999), "Experimental analysis and modelling of particle-wall collisions," *International Journal of Multiphase Flow*, **25**, 1457-1489
- UHLHERR, P.H.T., and SINCLAIR, C.G., (1970), "The effect of free-stream turbulence on the drag coefficient of spheres," *Proceedings of CHEMCA'70*, Butterworth of Australia and Institution of Chemical Engineers, 1-13
- WANG, Q., SQUIRES, K.D., and SIMONIN, O., (1998), "Large eddy simulation of turbulent gas-solid flows in a vertical channel and evaluation of second-order models," *International Journal of Heat and Fluid Flow*, **19**, 505-511